Available online at www.eccomasproceedia.org
Eccomas Proceedia SMART (2023) 2050-2059

ECCOMAS
Proceedia

X ECCOMAS Thematic Conference on Smart Structures and Materials
SMART 2023
D.A. Saravanos, A. Benjeddou, N. Chrysochoidis and T. Theodosiou (Eds)

INTEGRATION OF PZT THICK FILMS ON ADDITIVELY MANUFACTURED SUBSTRATES FOR VIBRATIONAL ENERGY HARVESTING APPLICATIONS

HELENE DEBEDA[†], NABIL ALAID[*], SHUO HE[*], BERNARD PLANO[†], EIHAB ABDEL-RAHMAN[*], ARMAGHAN SALEHIAN[*]

[†] Univ. Bordeaux, CNRS, Bordeaux INP, IMS, UMR 5218
F-33405 Talence Cedex, France
e-mail: helene.debeda@ims-bordeaux.fr, www.ims-bordeaux.fr/fr/

[*] Energy Harvesting and Vibrations Lab,
Mechanical and Mechatronics Engineering, and
Systems Design Engineering
University of Waterloo, Waterloo, ON, N2L 3G1, Canada
e-mail: salehian@uwaterloo.ca, https://uwaterloo.ca/

Abstract. The presented research is aimed at the integration of screen-printed thick films (50-100µm) of $PbZrTiO_3$ (PZT) on additively manufactured stainless steel substrates for vibration energy harvesting. The manufacturing technologies advanced by this research opens new horizons for energy harvesting applications as it standardizes the development and manufacturing processes, thereby making vibration energy harvesters more feasible. Since the parts are built layer-by-layer, the thickness of the different layers of the substrate can be controlled. The substrates under study were manufactured using Powder Bed Infusion additive manufacturing technology from Stainless Steel 17-4 PH powder. Simple cantilever harvesters are chosen as an initial target to focus on the optimization of the screen-printing process. The sample is 15.6 mm long, 4.1 mm wide and 0.35 mm thick cantilever beam with a 50µm thick PZT screen-printed layer sandwiched between two gold electrodes. A dielectric layer printed on the stainless steel substrate was introduced to promote adhesion. With 6.1mm of the beam length clamped and no tip mass the experimental resonant frequency was ~2kHz. The maximum output power was 39 nW under a resonant base acceleration with an amplitude of 0.3g at a load resistance of 100 kΩ. A good fit was found with a Finite Element Model with a difference of 5%. These initial results open routes for optimized designs of printed piezoelectric energy harvesters.

Key words: Screen Printing, Additive Manufacturing, Piezoelectric, Adhesion, Vibration Energy Harvester.

Peer-review under responsibility of the organizing committee of SMART 2023.
doi: 10.7712/150123.9973.451094

1 INTRODUCTION

With the increasing demand for autonomous electronic devices, vibratory piezoelectric energy harvesters are a promising option due to the availability of mechanical vibrations and the simplicity of electromechanical conversion. In this field, PZT ($PbZrTiO_3$) piezoelectric ceramics are studied because of their outstanding properties, despite the presence of lead in this material. For the manufacturing process of a high-performance piezoelectric ceramic, the main objectives are better densification, low manufacturing cost and integration in microgenerators.

For use in micro electromechanical systems (MEMS), thick piezoelectric elements are advantageous for high actuation forces or high power generation in MEMS applications [1]. Thin film technologies, such as sputtering, pulsed laser deposition and sol gel, require excessive deposition times and are limited in the maximum thickness obtainable due to the build-up of internal stresses during deposition which lead to film cracking [2]. On the other hand, the low cost thick-film screen printing PZT technology was already successfully applied for the fabrication of free-standing cantilever piezoelectric microsystems for sensor applications. The micro ceramics were composed of a PZT layer between two gold electrodes Au/PZT/Au [3]. Also for energy harvesting application, with a ceramic thick film of PZT integrated on a laser micromachined stainless steel (SS) resonant beam ($10x2x0.05mm^3$), interesting results were already obtained with a power of about 1µW measured at an acceleration of 0.5g and a frequency of 130Hz [2][4]. For complex passive substrate in energy harvesting, different manufacturing options can be found in the literature such as laser micromachining as in this study, and water jetting [5].

The presented research is aimed for the integration of PZT thick films (50-100µm) on additively manufactured samples stainless steel for vibrations energy harvesting applications. The manufacturing technologies to be adopted as part of this research opens new horizons for energy harvesting applications as it standardizes the development and manufacturing processes and make it more feasible to use the vibration energy harvesters. Since the parts are built layer-by-layer, the thickness of the different layers of the substrate can be controlled.

In this paper, the procedure of modeling and simulation of the selected cantilever beam is demonstrated. Then, the fabrication and printing process is explained in detail. Finally, the testing results are explained and analyzed and a comparison between the simulation and testing results under vibration is presented.

2 MODELING AND SIMULATION

2.1 Material properties

For this work, a new stainless steel substrate SS 17-4PH was considered for the substrate whose properties are compared with the SS301 used in previous study in table 1 [4]. Moreover, the material properties of the PZT used in the simulation are shown in table 2. These properties are obtained from previous experimental testing where printed thick films were used [6]. The greater the difference between the Coefficient of Thermal Expansion (CTE) of the substrate material and the one of the PZT is, the higher the chance is for delamination and adhesion issues. SS17-4 PH has a lower CTE compared to SS301. These reduced differences between

the CTE of SS17-4PH and the CTE of the top layer (PZT and Au) are hence assumed to offer better adhesion.

Table 1: Comparison between stainless steel substrate materials [6] [8]

	SS 301	**SS 17-4PH**
Young Modulus[GPa]	193	197
Density (kg/m^3)	7,880	7,780
Coefficient of Thermal Expanison (CTE) [ppm/°C]	18	8.1
Main additives	17 % chromium and 7 % nickel	17% chromium and 4% nickel

Table 2: Screen-printed PZT parameters [6]

Young's modulus	43 GPa
Density	5500 kg/m^3
Piezoelectric coefficient d_{31}	-40 pC/N
CTE	4.7 ppm/°C

2.2 Finite element analysis

The following procedure was followed to carry out the simulation starting from geometry creation with COMSOL Multiphysics followed by the eigen frequency analysis and finally the piezoelectric modelling. The beam consists of a section which is free to vibrate with a length of 9.5 mm, and section to be clamped for a length of 6.1 mm. The PZT layer of a thickness of 0.05 mm was added on top of the free section. In addition two electrodes of thickness of 0.01 mm at the top and bottom of the PZT layers were created.

The steps which followed the material definition are the following:

1. The substrate was assigned as the Linear Elastic Material and the PZT stripes was assigned as the Piezoelectric Layer,
2. The damping ratios were assigned for each material. As per the material properties, the value of damping ratio used for the substrate is 0.01, and the damping ratio used for the PZT layer is ζ=0.001,
3. The side to be clamped was assigned as a fixed constraint,
4. An acceleration of 0.3g was applied to the free side.

The Eigenfrequency study was achieved to determine the natural frequency and mode shapes. For power simulations with different loads a frequency domain study with resistance sweep was used.

3 FABRICATION

3.1 Additive manufacturing

The flexibility in changing the thickness to alter the natural frequency emphasizes the importance of using additive manufacturing technologies. Since the parts are built layer-by-layer, the thickness of the substrate can be controlled.

The Selective Laser Melting (SLM) technology available at MSAM Lab at Waterloo (https://msam.uwaterloo.ca/) whose specifications are given in table 3 was chosen. Compared to the Electron Beam Melting technique also proposed for metallic 3D printing, SLM is attractive because of the possibility to sinter at much lower temperatures (5-200 $^{\circ}$C) [8] and it is used to combine metals with high melting points.

In this 3D printing SLM process, the powder bed is in inert atmosphere to provide shielding of the molten metal. The laser beam is the energy source used to scan each layer of the already spread powder to selectively melt the material according to the part cross section obtained from the digital part model. When one layer has been scanned, the piston of building chamber goes down whereas the piston of the powder chamber goes up by defined layer thickness. The roller deposits powder across build chamber which is again scanned by the energy source. This cycle is repeated layer by layer, until the complete part is formed. The end result of this process is powder cake, and the part is not visible until excess powder is removed.

Table 3: Selective Laser Melting (SLM) Specifications [9] [10]

Power Source	**One or more fiber lasers of 200 to 1000W**
Build chamber environment	Argon or Nitrogen
Powder preheating temperature	100-200 (°C)
Maximum available build volume	500 x 350 x 300 mm^3
Maximum build rate	20-35 (cm^3/hr)

For the feasibility study a simple shaped substrate was 3D printed (15.6 mm long, 4.1 mm wide and 0.35 mm thick). After the 3D printing, the roughness *Ra* was about 6 µm. This was too high to further print layers with thicknesses of tens of micrometers. A manual polishing step with a fine sandpaper (P1200 ISO) was hence included to reduce the porosity *Ra* at around 0.5 to 1.9 µm.

3.2 Piezoelectric layer screen-printing

The screen-printing method is a low-cost alternative process to classical silicon manufacturing. This process requires specific inks, made of a mixture of powders and organic

binder to be transferred onto the substrate through open areas of meshes of the patterned screen by a squeegee. The deposited film, in the range of 5-100 µm, is then dried and fired to achieve sintering and adherence of the thick film on the substrate. The most valuable advantages of screen-printing are the low investment costs for equipment, choice of materials including the substrate and paste and the implementation of complex geometries. Our studied energy harvesting microsystem consists in a three-dimensional thick-film structure made of a thick PZT layer sandwiched between two gold electrodes deposited on the 3D manufactured stainless substrate (SS).

Figure 1 below summarizes the thick-film PZT screen printing process. The pressure step is an additional step in the process necessary to reduce porosity of the PZT layer [7].

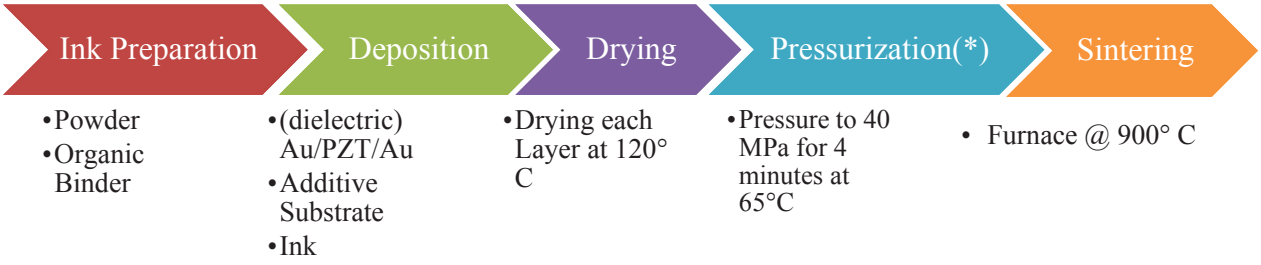

Figure 1 Steps of PZT Thick Film Screen Printing Process (*additionnal step in the standard process)

3.2.1. Pastes

The gold paste used for the electrodes is a commercially available paste provided by ElectroScience Laboratory (newly Ferro https://www.ferro.com/). It is named ESL8836 and it contains different oxides such as SiO_2, Al_2O_3, CdO, PbO that will help for the chemical bond on the stainless substrate [4]. In the case of unsatisfactory interfaces, a layer of ESL 4924 dielectric ink is proposed. This dielectric layer is non-porous and has been developed by ESL to closely matches most types of stainless steel.

The PZT powder (hard type PZ26 from Ferroperm) was mixed with the sintering aid powders Li_2CO_3, Bi_2O_3 and CuO (Sigma Aldrich) that help to lower the sintering temperature with a better densification and reproducibility of the thick film. The powder composition given table 4 was chosen according to the composition from [11].

All powders were first mixed in a Turbula, dried and a binder ESLV400 was then incorporated to the powder mix (~15%wt). The paste was then placed in a three-roll miller (EXAKT 80S) in order to evenly distribute the particles.

Table 4: PZT powder composition.

Powder	Wt. %	Mass (g)
PZT (PZ26 Ferroperm)	97.00	38.8
Li_2CO_3 (Sigma Aldrich)	0.80	0.32

Bi_2O_3 (Sigma Aldrich)	1.20	0.48
CuO (Sigma Aldrich)	1.00	0.40
Total:	100.00	40

3.2.2. Layer deposition and thermal treatment

The Fristch PrintALL 210 screen printer was used to deposit the thick films on the additive substrate (dielectric, Au electrode and PZT layers).

Mesh screens were selected to print all layers. It indeed offers wider flexibility in the design than a stencil that could also be used to print thick PZT layer (> 50µm). The following screen characteristics for the mesh screen and the expected thickness are given Table 5.

Table 5: The screen settings used to print the different layers on the samples

Layer	Photoresist thickness (µm)	Screen Type (Mesh Count)	Expected wet layer after printing
Dielectric Layer	15	325	30µm
Bottom Electrode	15	325	30µm
PZT	50	200	70 µm
Top Electrode	15	325	30µm

The dielectric (if needed), bottom electrode, PZT layer and top electrode were successfully printed with a 10 min drying at 120°C between each printing. For the PZT active piezoelectric layer, 2 layers were screen-printed to achieve layers thicker than 50µm after drying and sintering. A slow drying (1°C/min) was necessary for this PZT layer to avoid cracks in the layers. After deposition of all the layers, the samples were pressurized at 40 MPa for 4 minutes and at 65°C. This was done in an isostatic pressurization machine, outsourced to Exxelia-Pessac (https://exxelia.com/en/).

The samples were then all conventionally sintered with the following steps. The sample was heated up to 450 ºC at a heating ramp of 40 ºC/min. Then the sample was held at 450 ºC for 30 minutes to ensure complete organic binder decomposition. The sample was then heated to 900 ºC at a heat ramp of 20 ºC/min for the sintering process at 900 ºC for 2 hours. Then the sample was cooled at 20 ºC/min until room temperature.

3.3 Polarization

Polarization was conducted by heating the sample up to 280 °C, below the Curie temperature of PZT of ~330 ºC. Before heating the sample, nitrogen gas was pumped into the oven such that polarization can happen in an inert gas. At the polarization temperature, voltage was applied during 10min to the sample, and it was ensured that the current did not exceed the limit 0.010 mA. Then, the sample was then cooled at a constant rate with the voltage field being held until 100 ºC. The maximum applied field for the sample was 5 kV/mm.

4 CHARACTERIZATIONS

Microstructure and interfaces were observed by Scanning Electron Microscope (JEOL-JSM-6100). Cross-sectioned, polished and carbon coated samples were prepared for SEM analysis. The software ImageJ was used of porosity estimation. The layer's thickness and roughness was measured with a stylus profilometer (Model KLA-Tencor).

The dynamic behavior of the fabricated micro-structures was characterized thanks to a laser doppler vibrometer (Polytec MSA-500) and allowed the measurement of the micro-beam's resonant frequency and the mechanical deflection of the tip's beam.

For the power output measurement, a shaker (Modal Shop-2075E) drove the microcantilever into resonance. The resonant frequency of the tested samples was determined from conducting a frequency sweep to find the peak voltage. The acceleration was set at 0.3g. Different electrical load varying from sweep between 10 KΩ to 9 MΩ were connected between top and bottom electrodes.

Using the load voltage and resistance, the power output of the sample can be determined, with RMS voltage (V_L) produced by the harvester at the resonant frequency and R_l the resistive load connected to the harvester (it includes the 10kΩ input resistive load of the multimeter).

$$P = \frac{V_L^2}{R_L}$$

5 RESULTS AND DISCUSSION

5.1 Microstructure and interfaces

Initial tests with gold electrodes revealed delamination between the lower gold layer and the PZT layer (Figure 2). As in previous tests with SS301 steel, gold/steel bonding is possible due to the formation of an interdiffusion layer of about 20 μm. The residual porosity was measured at ~36% with ImageJ. To overcome the delamination problem, a dielectric layer was added. This dielectric layer has a double advantage:

- Excellent adhesion to steel and gold
- A CTE close to that of PZT, which limits the lateral mechanical stresses imposed by PZT during its sintering.

A cross-section of another sample printed with the same conditions as the tested sample is shown in figure 3. We note the thicknesses of the dielectric layer, piezoelectric PZT and gold layers as: ~10 μm, ~50μm and 6-8 μm respectively.

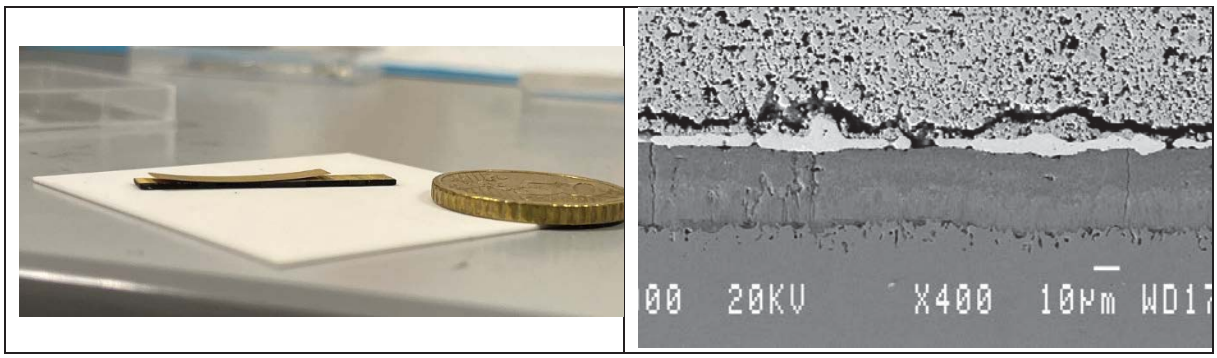

(a) (b)

Figure 2: Examples of delamination between bottom electrodes and PZT layers

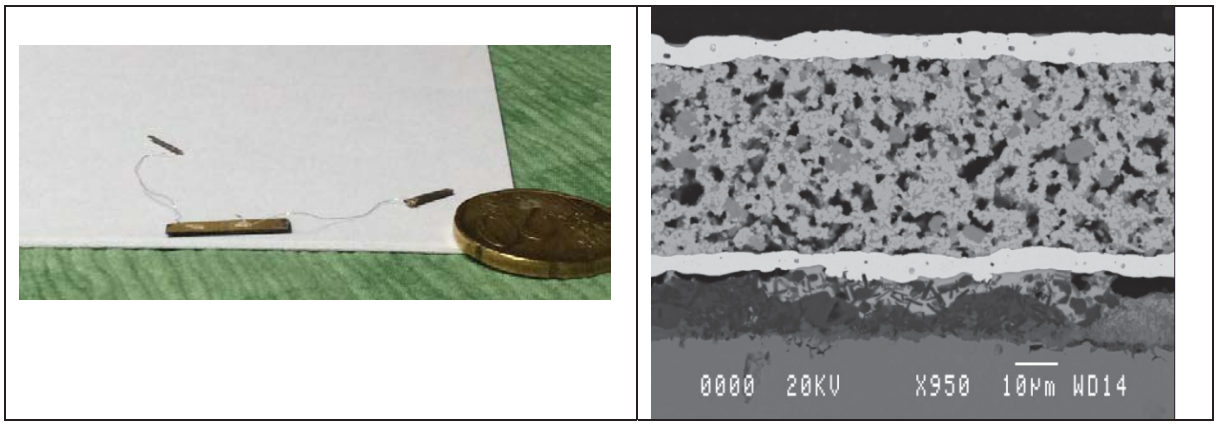

(a) (b)

Figure 3: (a) Photograph of a sample with gold and a dielectric layer (b) SEM cross section showing adhesion between layers after adding the dielectric layer

5.2 Vibrometer tests

A vibrometer was used to measure the tip displacement and the resonant frequency of the first flexural mode. Measurements were carried out before and after thermal treatment of the coated cantilevers. As a result of the sintering process, a drop in the resonant frequency was observed. It is attributed to a change in Young's modulus (Y) of the substrate due to exposure to high temperature for a long time. Based on the experiments, it was found that the natural frequency reduces after sintering by about 10% which corresponds to 19% reduction in the value of Young's Modulus to 157GPa. The reduced value was adopted in COMSOL modelling

5.3. Resonance frequency and power output

Figure 4 compares the experimental power output to COMSOL simulation results. A good match is observed between the two sets of results with a difference of less than 5%. The Normalized Power Density is found to be 28 $nW.g^{-2}.cm^{-3}$. The Power Density Value is lower than other harvesters used due to the size and the fact that the tip mass was not used.

The simulated natural frequency was found to be 2950 Hz. However, the experimental

natural frequency was found to be 2025 Hz. This difference is attributable to both non-ideal clamping conditions (clamping by screwing the beam extremity) and uncertainties in material properties (substrates and printed Au, dielectric and interdiffusion layers).

While the resonance frequency is too high for the purposes of vibration energy recovery, it can be reduced by increasing the length of the beam and adding a tip mass. For example, the addition of a 0.5 g tip mass reduces the simulated natural frequency by half to 1013 Hz and increases the power output to 118 nW.

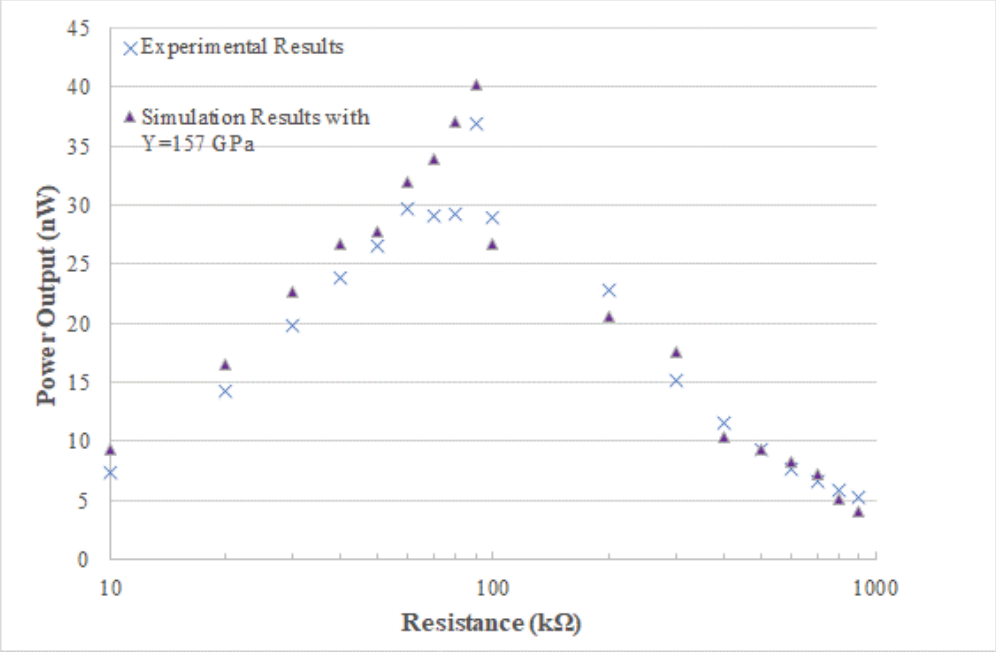

Figure 4: Measured and simulated power output under a base acceleration with a frequency matching the resonance frequency and an amplitude of 0.3 g

6 CONCLUSION

In this work, Au/PZT/Au layers were successfully printed using a low-cost screen-printing technology on a 3D printed stainless steel 17-4 PH additively manufactured by Selective Laser Melting SLM. The adhesion was good thanks to the use of a dielectric layer printed below the multilayer Au/PZT/Au. A residual porosity of ~36% was achieved similar to that of printed layers on SS301. The PZT was polarized and the maximum power output was 39 nW at an acceleration amplitude of 0.3g at a load resistance of 100 kΩ. The Normalized Power Density was 28 $\mu W.g^{-2}.cm^{-3}$. Simulation also confirmed that the introduction of a 0.5g tip mass to the harvester reduces the natural frequency to 1013 Hz and increases the power output to 118 nW. These initial results open routes for optimized designs for printed piezoelectric energy harvesters.

ACKNOWLEDGEMENTS

- Funded in part by the Marie Skłodowska-Curie Actions (MSCA) Research and Innovation Staff Exchange (RISE) H2020-MSCA-RISE-2018- 823895 'SENSOFT'.
- Dr. Salehian's UW International Research Partnership Grant.

REFERENCES

[1] C. Hindrichsen, R. Lou-Moeller, K. Hansen, E. Thomsen, 2010, "Advantages of PZT thick film for MEMS sensors", *Sensors and Actuators* A 163 (1) pp.9–14

[2] María Isabel Rua Taborda," Printed ceramic Piezoelectric MEMS for Energy Harvesting: towards Spark Plasma Sintering of multilayers, " Ph.D. dissertation, Mech. Eng.,Univ. of Bordeaux, Bordeaux, France, 2019.

[3] H. Debéda, P. Clément, E. Llobet, C. Lucat, "One-step firing for electrode PZT thick-films applied to MEMS", *Smart Mater. Struct.* 24, 2015, 025020

[4] Rua Taborda, M-I ; Elissalde, C. ; Chung, U-C ; Maglione, M. ; Fernandes, E.; Salehian, A., Santawitee, O. Debéda, H, "Key features in the development of unimorph Stainless Steel cantilever with screen-printed PZT dedicated to energy harvesting applications", *International Journal of Applied Ceramic Technology*, Wiley, 2020, 17 (6), pp.2533-2544. doi.10.1111/ijac.13588 Scopus

[5] M. Ibrahim, A.Salehian. "Modeling, fabrication, and experimental validation of hybrid piezo-magnetostrictive and piezomagnetic energy harvesting units". The Journal of Intelligent Materials Systems and Structures, Volume 26, issue 10. 2014.

[6] E. Fernandes, B. Martin, I. Rua, S. Zarabi, H. Debéda, D. Nairn, Lan Wei, A. Salehian, "Design, Fabrication, and Testing of a Low Frequency MEMS Piezoelectromagnetic Energy Harvester," *Smart Materials and Structures*, Volume 27, Number 3, Feb. 2018.

[7] H. Debéda, C. Lucat and F. Ménil, 2005, "Influence of the densification parameters on screen-printed component properties", *Journal of European Ceramic Society*, 25, 12, pp.2115-2119,

[8] Ian Gibson, David Rosen, Brent Stucker, Additive Manufacturing Technologies, 2nd edition, New York, USA, Springer, 2015

[9] GE Additive, Inside Electron Beam Melting, https://www.ge.com/additive/ebm

[10] B. Wysocki, P. Maj, R. Sitek, Joseph Buhagiar, K.J. Kurzydłowski, W. Swieszkowski, "Laser and Electron Beam Additive Manufacturing Methods of Fabricating Titanium Bone Implants," *Applied Sciences,* 2017, 657.

[11] Lakhmi, R., Debeda, H., Dufour, I., Lucat, C. and Maglione, M. (2014), Study of Screen-Printed PZT Cantilevers Both Self-Actuated and Self-Read-Out. *Int. J. Appl. Ceram. Technol.*, 11: 311-320. https://doi.org/10.1111/ijac.12006